proteins in an attempt to distinguish between deprotonation (Figure 1, 2 → 3) and H-atom abstraction (1 → 3 or 2 → 4) mechanisms. The recent model studies of Dinnocenzo and Banach,[14] however, have shown that all of these proteins N-dealkylate tertiary aromatic amines via deprotonation. The magnitude of the isotope effect is controlled by the nature of the proton-accepting distal base at the active site.[14] The peroxidases have a histidine proton donor/acceptor within their more polar active site regions,[2c,15] while cytochrome P-450 has a very nonpolar active site.[16,17] Small isotope effects (~2), therefore, rule out hydrogen radical abstraction events,[18] while large isotope effects (~9) may be due to deprotonation, H-atom abstraction, or H-atom tunneling.[9b,10] Miwa et al. reported (Table I) large isotope effects for heme proteins having histidine N-donor proximal ligands and small values for cysteinate S-donor ligated heme enzymes. Catalase, with a tyrosinate O-donor axial ligand, exhibited an intermediate value.[13] The present results clearly show that the identity of the proximal ligand is not a factor in determining the magnitude of the isotope effect. Instead, the value of the isotope effect for N-dealkylation by secondary amine monooxygenase of 1.76 is consistent with a deprotonation mechanism involving a P-450-like proton donor/acceptor environment.

(14) Dinnocenzo, J. P.; Banach, T. E. *J. Am. Chem. Soc.* **1989**, *111*, 8646-8653.
(15) Hawkins, B. K.; Dawson, J. H. *Frontiers in Biotransformation* in press.
(16) Poulos, T. N.; Finzel, B. C.; Howard, A. J. *J. Mol. Biol.* **1987**, *195*, 687.
(17) (a) Imai, M.; Shimada, H.; Watanabe, Y.; Matshushima-Hibiya, Y.; Makino, R.; Koga, H.; Horiuchi, T.; Ishimura, Y. *Proc. Natl. Acad. Sci. U.S.A.* **1989**, *86*, 7823-7827. (b) Martinis, S. A.; Atkins, W. M.; Stayton, P. S.; Sligar, S. G. *J. Am. Chem. Soc.* **1989**, *111*, 9522-9523.
(18) (a) Hull, I. A.; Davis, G. T.; Rosenblatt, D. H.; Williams, H. K. R.; Weglein, R. C. *J. Am. Chem. Soc.* **1967**, *89*, 1163-1170. (b) Lewis, F. D.; Ho, T. I. *J. Am. Chem. Soc.* **1980**, *102*, 1751-1752. (c) Lindsay Smith, J. R.; Masheder, D. *J. Chem. Soc., Perkin Trans. II* **1976**, 47-51. (d) Wei, M. M.; Stewart, R. *J. Am. Chem. Soc.* **1966**, *88*, 1974-1979.

Conclusion

In summary, secondary amine monooxygenase appears to catalyze N-demethylation reactions of secondary amines via a deprotonation, rather than an H-atom abstraction, limiting mechanism. Despite their different heme ligation, secondary amine monooxygeanse catalyzes oxidative N-dealkylation reactions by a mechanism like that employed by the only other heme-containing monooxygenase, cytochrome P-450. Thus, the nature of the proximal axial ligand is not a controlling factor in determining the mechanism of N-dealkylation. Furthermore, the distal proton donor/acceptor characteristics of these two proteins appear to be similar.

Acknowledgment. We are grateful for NIH GM-26730, Sigma Xi. B.K.H. thanks Rohm and Haas, Inc. for a fellowship. We thank Dr. Mike Walla for technical assistance; Drs. Ronald E. White, Masanori Sono, Alfin Vaz, and David Wink for helpful discussions; and Dr. J. R. Durig, University of South Carolina for the kind gift of 1,1,1-trideuteriodimethylamine·HCl.

Registry No. D_2, 7782-39-0; H_3C-NH-CH_3, 124-40-3; secondary amine monooxygenase, 37367-72-9.

Developing Magnetic and Metallic Behavior in High-Nuclearity Nickel Cluster Carbonyls. A LCGTO-LDF Study of $[Ni_9(CO)_{18}]^{n-}$, $[Ni_{10}Ge(CO)_{20}]^{n-}$, $[Ni_{32}C_6(CO)_{36}]^{n-}$, and $[Ni_{44}(CO)_{48}]^{n-}$ Compounds

Notker Rösch,*,† Lutz Ackermann,† and Gianfranco Pacchioni*,‡

Contribution from the Lehrstuhl für Theoretische Chemie, Technische Universität München, 8046 Garching, Germany, and Dipartimento di Chimica Inorganica e Metallorganica, Università di Milano, Centro CNR, via Venezian 21, 20133 Milano, Italy. *Received August 27, 1991*

Abstract: We have performed all-electron calculations on the electronic structure of medium- and high-nuclearity bare and carbonylated nickel cluster compounds by means of the linear combination of Gaussian type orbitals (LCGTO) local density functional (LDF) method. The transition from the molecular state to the metallic state as a function of the cluster size was studied by determining the one-electron energy spectra and the magnetic properties of naked and ligated Ni clusters. Medium-size clusters like $[Ni_9(CO)_{18}]^{2-}$ and $[Ni_{10}Ge(CO)_{20}]^{2-}$, where all the Ni atoms are on the surface of the metal cage, show typically molecular features. They do not exhibit any magnetic behavior, and their one-electron spectrum has a discrete nature near the cluster HOMO with a well-defined HOMO–LUMO gap. By contrast, both high-nuclearity clusters, $[Ni_{32}C_6(CO)_{36}]^{n-}$ and $[Ni_{44}(CO)_{48}]^{n-}$, show typical signs of a developing metallic character in agreement with experimental magnetic measurements. In particular, a magnetic behavior connected with the high density of states near the Fermi level is observed. This is entirely connected to the presence of Ni atoms in the interior ("bulk") of the metal cage. The role of the CO ligands and of interstitial atoms, like C or Ge, in quenching the magnetic moment of the bare cluster is elucidated.

1. Introduction

The study of compounds involving transition metal clusters has been one of the most rapidly expanding areas within inorganic and organometallic chemistry in recent years.[1] Most clusters share common framework structures in which metal atoms form a close-packed array; the largest class is composed of clusters in which all the atoms are formally zero-valent and the associated ligands have substantial π-acceptor character, as in metal carbonyl

* To whom correspondence should be addressed.
† Technische Universität München.
‡ Università di Milano.

(1) (a) Moskovits, M., Ed. *Metal Clusters*; Wiley: New York, 1986. (b) Mingos, D. M. P.; Wales, D. J. *Introduction to Cluster Chemistry*; Prentice Hall: London, 1990. (c) Schmid, G. *Struct. Bonding (Berlin)* **1985**, *62*, 51.

0002-7863/92/1514-3549$03.00/0

clusters.[1] For years, the main focus has been on the possible use of molecular clusters as efficient catalysts.[2] This idea was based on the similarity of metal–ligand bonding in cluster compounds with the chemisorption of small molecules at solid surfaces;[3] in this respect, clusters represent very useful molecular synthetic analogues of chemisorption systems. However, it is now well established that molecular clusters as such are, with few exceptions, poor homogeneous catalysts because of their high stability and their relatively strong metal–ligand bonds. On the contrary, metal cluster compounds have been successfully employed as starting materials for obtaining highly reactive surface species upon deposition on inert materials like zeolites, silica, or alumina followed by thermal treatment.[4]

Only recently, the large body of structural and chemical information achieved in 20 years of chemical research on clusters has stimulated the study of the physical properties of this new class of materials.[5] From a solid state chemistry point of view, ionic cluster compounds crystallized into regular lattice structures with suitable counterions form "cluster solids" exhibiting some analogies with the Chevrel phases. A major difference is that the building blocks, which in Chevrel phases are typically octahedral clusters of six Mo (or Re, Ru) atoms surrounded by a cube of S (or Se, Te) atoms, are here replaced by metal cluster cores with various structures. One notes the analogy that both types of materials can be viewed as assemblies of identical metal particles embedded in the dielectric matrix formed by the ligands and the counterions.

The existence of cluster compounds of increasing size offers the possibility of investigating experimentally the evolution of metallic properties as the size of the metal particle grows. Measurements of macroscopic properties like magnetization, susceptibility, electrical conductivity, etc., have been performed on several molecular clusters in combination with microscopic probes such as NMR, ESR, and Mössbauer measurements.[5] Substantial deviations have been observed in the physical properties of cluster compounds from those of the corresponding bulk metals. In particular, while small molecular clusters containing 10 or less metal atoms usually do not exhibit magnetic behavior, medium-size clusters, typically of 20–40 atoms, exhibit a magnetization which is 5–10 times smaller than in the corresponding metals.[5f,g] X-ray photoelectron spectroscopy and Mössbauer measurements of high-nuclearity cluster compounds show significant similarities with the bulk metals which are indicative of a developing metallic character.[5g]

From a theoretical point of view, molecular metal clusters represent a unique class of compounds intermediate between the molecular and the solid state. The study of the transition from the discrete one-electron energy levels of mononuclear organometallic complexes to the "dense" one-electron spectrum of high-nuclearity metal clusters is a fascinating subject but also a formidable challenge to theoretical methods. Most of the theoretical studies on cluster compounds are based on simplified approaches which have value for the qualitative rationalization of the chemistry of these systems, but which are inadequate for the detailed understanding of their electronic properties.[6]

Among these properties, magnetic properties are very important for determining the "molecular" or "metallic" nature of the cluster. Recently, semiempirical[7] as well as local density[8,9] calculations on "small" carbonylated clusters have shown that the main effect of the ligand coordination to the metal core is to redistribute electrons around the cluster Fermi level, or cluster HOMO. The sp-derived levels become less energetically favorable, and electrons move from the sp- to the d-type levels with concomitant quenching of the initial magnetic moment of the bare metal particle. Similar local quenching effects occur upon chemisorption of CO on the surface of magnetic materials.[10-14] This is in many respects analogous to crystal field effects exerted by the ligands on a single metal atom. We have recently proposed that the total magnetic quenching in the small clusters is the direct consequence of the fact that all the metal atoms are surface atoms which are directly bonded with the CO ligands.[9] In order to observe the development of a metallic (magnetic) character, larger cluster compounds containing at least some metal atoms with a bulklike coordination are needed.

In this paper we have extended our previous work on small-size $[Ni_5(CO)_{12}]^{2-}$, $[Ni_6(CO)_{12}]^{2-}$, and $[Ni_8C(CO)_{16}]^{2-}$ clusters[9] to medium- and large-size carbonylated Ni clusters in order to verify the hypothesis mentioned above. We have performed linear combination of Gaussian-type orbitals (LCGTO) local density functional (LDF) calculations on two medium-size clusters, $[Ni_9(CO)_{18}]^{2-}$ with a layered structure[15] and $[Ni_{10}Ge(CO)_{20}]^{2-}$ with an interstitial Ge atom,[16] and on two large systems, $[Ni_{32}C_6(CO)_{36}]^{n-}$ and $[Ni_{44}(CO)_{48}]^{n-}$ (n = 0, 2, 4, 6). The cluster structures have been taken from experimental X-ray data. The two larger clusters are idealized models of two parent compounds. The structure of $[Ni_{32}C_6(CO)_{36}]^{n-}$ is derived from that of $[Ni_{38}C_6(CO)_{42}]^{6-}$ by eliminating six Ni–CO groups capping some of the faces of the regular Ni_{32} polyhedron.[17] The structure of $[Ni_{44}(CO)_{48}]^{n-}$ has been derived from that of $[Ni_{38}Pt_6(CO)_{48}]^{n-}$ by replacing the six internal Pt atoms with Ni atoms.[18] The largest cluster, $[Ni_{44}(CO)_{48}]^{n-}$, contains more than 1900 electrons; the calculation of the wavefunction for $[Ni_{44}(CO)_{48}]^{n-}$ is a major effort since about 3.300 contracted basis functions are needed to

(2) Muetterties, E. A.; Krause, M. J. *Angew. Chem., Int. Ed. Engl.* **1983**, *22*, 135.

(3) (a) Muetterties, E. L.; Rhodin, T. N.; Band, N.; Brucker, C. F.; Pretzer, W. R. *Chem. Rev.* **1979**, *79*, 91. (b) Muetterties, E. L.; Wexler, R. M. *Survey of Progress in Chemistry*; Academic Press: New York, 1983; Vol. 10, p 61. (c) Albert, M. R.; Yates, J. R. *The Surface Scientist's Guide to Organometallic Chemistry*, American Chemical Society: Washington, DC, 1987.

(4) (a) Gates, B. C., Guczi, L., Knözinger, H., Eds. *Metal Clusters in Catalysis*; Elsevier: Amsterdam, 1986. (b) Zwart, J.; Snel, R. *J. Mol. Catal.* **1985**, *30*, 305.

(5) (a) Benfield, R. E.; Edwards, P. P.; Stacy, A. M. *J. Chem. Soc., Chem. Commun.* **1982**, 526. (b) Johnson, D. C.; Benfield, R. E.; Edwards, P. P.; Nelson, W. J. H.; Vargas, M. D. *Nature* **1985**, *314*, 231. (c) Teo, B. K.; DiSalvo, K. J.; Waszczak, J. W.; Longoni, G.; Ceriotti, A. *Inorg. Chem.* **1986**, *25*, 2262. (d) Pronk, B. J.; Brom, H. B.; de Jongh, L. J.; Longoni, G.; Ceriotti, A. *Solid State Commun.* **1986**, *59*, 349. (e) van Staveren, M. P. J.; Brom, H. B.; de Jongh, L. J.; Schmid, G. *Solid State Commun.* **1986**, *60*, 319. (f) de Jongh, L. J.; de Aguiar, J. A. O.; Brom, H. B.; Longoni, G.; van Ruitenbeek, J. M.; Schmid, G.; Smit, H. H. A.; van Staveren, M. P. J.; Thiel, R. C. *Z. Phys. D* **1989**, *12*, 445. (g) de Jongh, L. J.; Brom, H. B.; van Ruitenbeck, J. M.; Thiel, R. C.; Schmid, G.; Longoni, G.; Ceriotti, A.; Zanoni, R. In *Cluster Models for Surface and Bulk Phenomena*; Pacchioni, G., Bagus, P. S., Parmigiani, F., Eds.; NATO ASI Series B; Plenum: New York, in press.

(6) (a) Dedieu, A.; Hoffmann, R. *J. Am. Chem. Soc.* **1978**, *100*, 2074. (b) Evans, D. G.; Mingos, D. M. P. *Organometallics* **1983**, *2*, 435. (c) Halet, J. F.; Hoffmann, R.; Saillard, J. Y. *Inorg. Chem.* **1985**, *24*, 1695. (d) Underwood, D. J.; Hoffmann, R.; Tatsumi, K.; Nakamura, A.; Yamamoto, Y. *J. Am. Chem. Soc.* **1985**, *107*, 5968. (e) Lauher, J. W. *J. Am. Chem. Soc.* **1978**, *100*, 5305. (f) *Ibid.* **1979**, *101*, 2604. (g) Mingos, D. M. P.; Johnston, R. L. *Struct. Bonding (Berlin)* **1987**, *68*, 29. (h) Rives, A. B.; Xiao-Zeng, Y.; Fenske, R. F. *Inorg. Chem.* **1982**, *21*, 2286. (i) Pacchioni, G.; Fantucci, P.; Valenti, V. *J. Organomet. Chem.* **1982**, *224*, 89. (j) Fantucci, P.; Pacchioni, G.; Valenti, V. *Inorg. Chem.* **1984**, *23*, 247.

(7) (a) Pacchioni, G.; Fantucci, P. *Chem. Phys. Lett.* **1987**, *134*, 407. (b) Pacchioni, G. In *Elemental and Molecular Clusters*; Benedek, G., Martin, T. P., Pacchioni, G., Eds.; Springer: Berlin, 1988.

(8) Holland, G. F.; Ellis, D. E.; Trogler, W. C. *J. Chem. Phys.* **1985**, *83*, 3507.

(9) Pacchioni, G.; Rösch, N. *Inorg. Chem.* **1990**, *29*, 2901.

(10) Selwood, P. W. *Chemisorption and Magnetization*; Academic Press: New York, 1975.

(11) Feigerle, C. S.; Seiler, A.; Pena, J. I.; Celotta, R. J.; Pierce, D. T. *Phys. Rev. Lett.* **1986**, *56*, 2207.

(12) Rösch, N.; Knappe, P.; Sandl, P.; Görling, A.; Dunlap, B. I. In *The Challenge of d and f Electrons. Theory and Computations*; Salahub, D. R., Zerner, M. C., Eds.; ACS Symposium Series 394; American Chemical Society: Washington, DC, 1989; p 180.

(13) Raatz, F.; Salahub, D. R. *Surf. Sci.* **1986**, *176*, 219.

(14) Bauschlicher, C. W.; Nelin, C. J. *J. Chem. Phys.* **1986**, *108*, 275.

(15) Nagaki, D. A.; Lower, L. D.; Longoni, G.; Chini, P.; Dahl, L. F. *Organometallics* **1986**, *5*, 1764.

(16) Ceriotti, A.; Demartin, F.; Heaton, B. T.; Ingallina, P.; Longoni, G.; Manassero, M.; Marchionna, M.; Masciocchi, N. *J. Chem. Soc., Chem. Commun.* **1989**, 786.

(17) Ceriotti, A.; Fait, A.; Longoni, G.; Piro, G. *J. Am. Chem. Soc.* **1986**, *108*, 8091.

(18) Ceriotti, A.; Demartin, F.; Longoni, G.; Manassero, M.; Marchionna, M.; Piva, G.; Sansoni, M. *Angew. Chem., Int. Ed. Engl.* **1985**, *24*, 697.

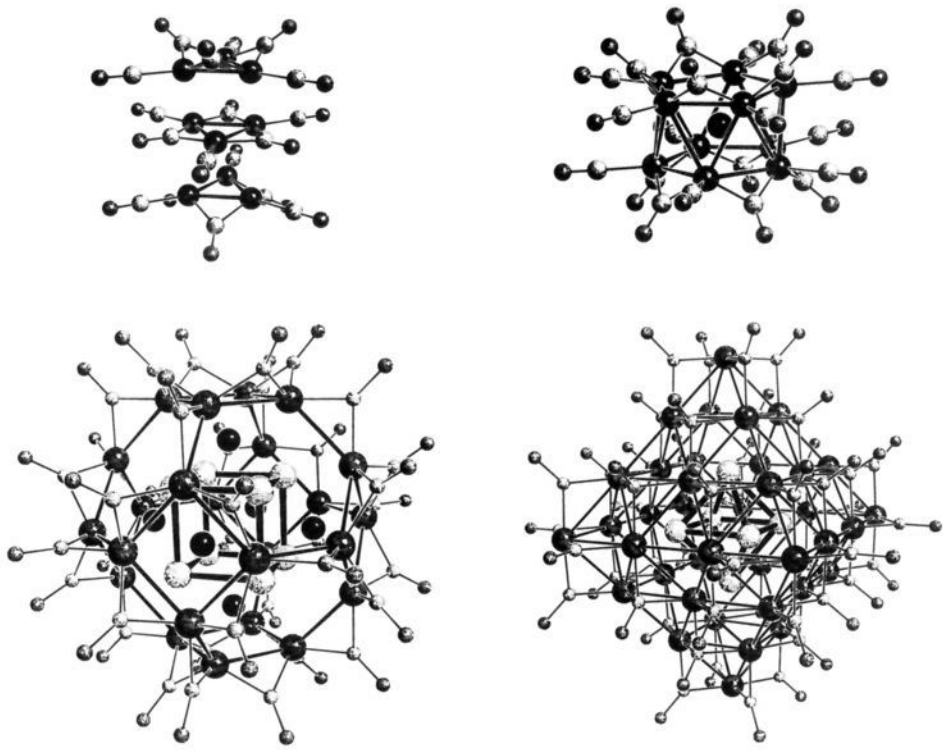

Figure 1. Geometry of the $[Ni_9(CO)_{18}]^{2-}$, $[Ni_{10}Ge(CO)_{20}]^{2-}$, $[Ni_{32}C_6(CO)_{36}]^{n-}$, and $[Ni_{44}(CO)_{48}]^{n-}$ clusters. In $[Ni_9(CO)_{18}]^{2-}$, D_{3h} symmetry was assumed. The intra- and interunit Ni–Ni distances were fixed at the average experimental values,[15] 2.38 and 2.77 Å, respectively. D_{5d} symmetry was assumed for the $[Ni_{10}Ge(CO)_{20}]^{2-}$ cluster. The intra- and interunit distances were fixed at the average experimental values,[16] 2.55 and 2.72 Å, respectively. O_h symmetry was assumed for both clusters $[Ni_{32}C_6(CO)_{36}]^{n-}$ and $[Ni_{44}(CO)_{48}]^{n-}$. In Ni_{32}, the intermetallic distances used are 2.40 Å (inner cube, light shading) and 2.46 Å (outer cage, dark shading); the nearest neighbor distance between inner and outer Ni atoms is 2.63 Å.[17] In Ni_{44}, the Ni–Ni distance was fixed at the average experimental value 2.58 Å.[18] For all clusters the following distances were taken: Ni–CO (terminal), 1.75 Å; Ni–CO (bridge), 1.90 Å; C–O (terminal), 1.13 Å; C–O (bridge), 1.17 Å.

Table I. Distances, r (Å), Total Energy, E_T (au), Dissociation Energy per Atom, D_e/n (kJ/mol), Fermi Energy, ϵ_F (eV), Total, N_s, and Average, n_s, Numbers of Unpaired Electrons per Ni Atom in Bare Ni Clusters

cluster	r_1, r_2[a]	E_T	$D_e(n+m)$[b]	ϵ_F	N_s	n_s
Ni_3	2.38	−4518.1619	134	−2.93	2.47	0.82
Ni_9	2.38, 2.77	−13554.7988	225	−3.27	8.11	0.90
Ni_{10}	2.55, 2.72	−15060.9133	232	−3.47	8.79	0.88
$Ni_{10}Ge$	2.55, 2.72	−17119.5795	273	−3.48	5.58	0.56
Ni_{32}	2.40, 2.46, 2.63	−48196.9760	400	−3.73	26.44	0.83
$Ni_{32}C_6$	*2.40, 2.46, 2.63*	*−48422.9708*	*477*	*−3.77*	*10.13*	*0.32*
Ni_{44}	2.58	−66270.7531	395	−3.71	32.66	0.74

[a] r_1 and r_2 are the nearest and next-nearest neighbor distances. See also Figure 1. [b] Dissociation energy computed as $[-E(Ni_nX_m) + nE(Ni) + mE(X)]/(n+m)$; $E(Ni;^3D(3d^94s^1)) = -1506.0030$ au; $E(C;^2P(2s^22p^2)) = -37.3288$ au); $E(Ge;^2P(4s^24p^2)) = -2058.4063$ au.)

represent its molecular orbitals.

2. Computational Details

In the LCGTO-LDF method, one solves effective one-electron equations derived in the Kohn–Sham approach to density functional theory[19]

$$[-\tfrac{1}{2}\nabla^2 + \nu(r)]\psi_i(r) = \epsilon_i\psi_i(r)$$

Here, the local potential ν contains the electron–nucleus attraction, the classical interelectronic repulsion from the charge density

$$\rho(r) = \sum n_i|\psi_i(r)|^2$$

and the exchange-correlation potential $\nu_{xc}(r)$, which in the present study was taken in the form

$$\nu_{xc}(r) = -(3/2)\alpha[(3/\pi)\rho(r)]^{1/3}$$

with the parameter α set to 0.7. A generalization of the formalism to a spin-polarized version was used to describe systems with unpaired electrons.[19-21] A fundamental characteristic of the LCGTO-LDF approach[12,20,21] is the use of three different Gaussian-type basis sets for the description of the Kohn–Sham orbitals, for the approximation of the charge density

$$\rho(r) \approx \bar{\rho}(r) = \sum a_i f_i(r)$$

and of the exchange-correlation potential

$$\nu_{xc}(r) \approx \nu_{xc}(r) = \sum b_i g_i(r)$$

The coefficients a_i are determined variationally by minimizing the Coulomb self-interaction of the difference $\Delta\rho = \rho - \bar{\rho}$. From a least-squares procedure over a moderate-size grid of points one obtains the expansion coefficients b_i. For Ni, C, and O the same contracted basis set employed for the previous study was used here.[9] For Ge a [20s,14p,9d/9s,7p,3d] basis set was used.[22]

In metallic clusters, one often finds that there are very many one-electron energy levels near the HOMO–LUMO gap resulting in a manifold of configurations that are energetically very close to the ground state. In this case, a convenient strategy is to aim at a suitable average over this manifold of close-lying states leading to fractional occupation numbers n_i of the one-electron levels.[12,23] To this end, one formally

(19) Parr, R. G.; Yang, W. *Density Functional Theory of Atoms and Molecules*; Oxford University Press: New York, 1989.
(20) Dunlap, B. I.; Rösch, N. *J. Chim. Phys. Phyis.-Chim. Biol.* **1989**, *86*, 671.
(21) Dunlap, B. I.; Rösch, N. *Adv. Quantum Chem.* **1990**, *21*, 317.
(22) Huzinaga, S.; Klobukowski, M. *J. Mol. Struct. (THEOCHEM)* **1988**, *167*, 1.

Table II. Total Energy, E_T (au), of Neutral and Negatively Charged Ni Clusters

cluster	E_T			
	$n = 0$	$n = 2$	$n = 4$	$n = 6$
$[Ni_3(CO)_6]^{n-}$	-5191.4400	-5191.3950		
$[Ni_9(CO)_{18}]^{n-}$	-15574.3972	-15574.5410		
$[Ni_{10}Ge(CO)_{20}]^{n-}$	-19363.6149	-19363.7451		
$[Ni_{32}C_6]^{n-}$	-48 422.9137	-48 422.9936	-48 422.6922	-48 422.0280
$[Ni_{32}(CO)_{36}]^{n-}$	-52 235.9776	-52 236.2026	-52 236.0622	-52 235.5739
$[Ni_{32}C_6(CO)_{36}]^{n-}$	-52 461.8777	-52 462.0581	-52 461.9373	-52 461.4627
$[Ni_{44}(CO)_{48}]^{n-}$	-71 652.4643	-71 652.7078	-71 652.6216	-71 652.2143

broadens each one-electron level by a Gaussian and fills the resulting density of states (DOS) up to a cluster Fermi energy which is determined self-consistently. We have employed this technique for naked and carbonylated Ni clusters.[9]

All calculations have been carried out on a CONVEX C210 computer.

3. Results and Discussion

3.1. The Cluster $[Ni_9(CO)_{18}]^{2-}$. Both neutral and dianionic forms of the $Ni_9(CO)_{18}$ cluster have been considered. This cluster consists of three $Ni_3(CO)_6$ building blocks with large interplanar Ni–Ni distances, about 2.7 Å (Figure 1). It may be viewed as an extension of the cluster $[Ni_6(CO)_{12}]^{2-}$ by a third $Ni_3(CO)_6$ unit. We have shown[9] that one of the major consequences of the carbonylation of a bare metal particle is the weakening of the Ni–Ni bonds. This conclusion is supported by considerable evidence, including the analysis of the electron density difference contour maps.[9] Here we provide additional arguments based on the energetics of the following reactions (see Tables I and II):

$$3Ni_3 \rightarrow Ni_9 \qquad \Delta E = -822 \text{ kJ/mol}$$

$$3Ni_3(CO)_6 \rightarrow Ni_9(CO)_{18} \qquad \Delta E = -203 \text{ kJ/mol}$$

$$3Ni_3(CO)_6 + 2e^- \rightarrow [Ni_9(CO)_{18}]^{2-} \qquad \Delta E = -580 \text{ kJ/mol}$$

The bare Ni_9 cluster is very stable with respect to dissociation in Ni_3 units, despite the large interunit Ni–Ni distance. (The geometry of the bare cluster is always assumed to be that of the corresponding carbonylated species.) The fully carbonylated neutral cluster exhibits only a moderate stability with respect to fragmentation into the monomeric $Ni_3(CO)_6$ units. On the other hand, addition of two extra electrons has the effect of considerably stabilizing the structure. In the crystal, further stabilization comes from the electrostatic interaction with the counterions. Similar conclusions have been reached previously[9] for the dimerization of $Ni_3(CO)_6$ to give the $Ni_6(CO)_{12}$ cluster. Taken altogether, these data show that the addition of the 18 CO ligands to the bare metal cluster reduces the interunit bonding; the stability of the complex is partly restored in its anionic form. The two extra electrons fill an orbital with a large Ni 4sp-component which fosters the bonding between the Ni_3 planes, in analogy with the dimeric $[Ni_6(CO)_{12}]^{2-}$ form.[9]

The cluster $[Ni_9(CO)_{18}]^{2-}$ is diamagnetic, as expected on the basis of our previous results.[9] It exhibits a HOMO–LUMO gap of about 2 eV. The DOS curve (Figure 2), obtained by broadening the discrete one-electron energy levels with a Gaussian function of fixed half-width 0.1 eV, shows the typical features found for smaller clusters: a filled d-band below the Fermi level, with the Ni s-type and the CO $2\pi^*$ levels well above it. This indicates the "molecular" nature of this cluster, which lacks any metallic character.

3.2. The Cluster $[Ni_{10}Ge(CO)_{20}]^{2-}$. This cluster consists of a Ni_{10} pentagonal antiprism with an interstitial Ge atom at its center. Thus, the Ge atom may directly interact only with the Ni atoms, while all the Ni atoms are on the surface of the cluster (Figure 1). The bare Ni_{10} cluster with no interstitial atom exhibits a high magnetization, 8.8 unpaired electrons. This corresponds to an average magnetization of about 0.9 unpaired electrons per Ni atom, which is considerably larger than the value of 0.6 μ_B found for bulk Ni.[24] This is a consequence of the large distance between

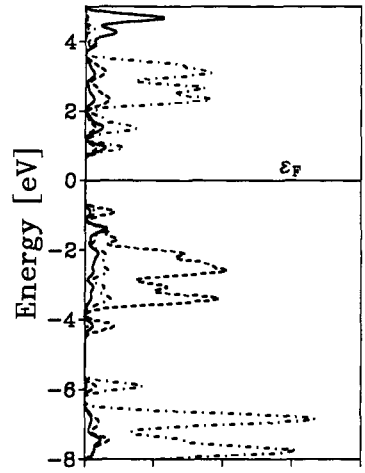

Figure 2. $[Ni_9(CO)_{18}]^{2-}$ density of states (in arbitrary units) generated by Gaussian broadening of the one-electron energies (non-spin polarized calculation): – –, Ni 3d contribution; —, Ni 4s–4p contribution; –·–, contribution of the CO orbitals. ϵ_F indicates the cluster Fermi energy (the cluster HOMO).

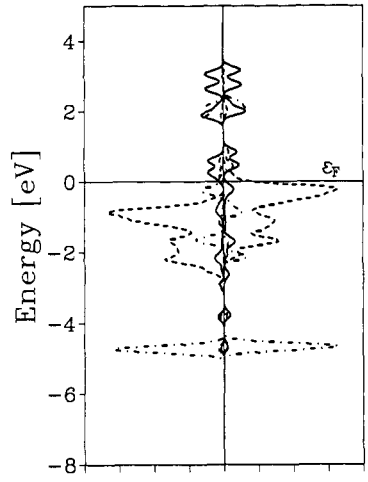

Figure 3. $Ni_{10}Ge$ density of states (in arbitrary units) generated by Gaussian broadening of the one-electron energies (spin polarized calculation, left side minority spin, right side majority spin): – –, Ni 3d contribution; —, Ni 4s–4p contribution; –·–, contribution (×10) of the Ge orbitals. ϵ_F indicates the cluster Fermi energy.

the two pentagonal Ni_5 units and of the low coordination number of the Ni atoms in the cluster as compared to the bulk. The addition of the central Ge atom stabilizes the whole structure with respect to fragmentation by about 680 kJ/mol and reduces the total magnetic moment to 5.6 unpaired electrons (Table I). The bare $Ni_{10}Ge$ cluster has typical metallic features, as shown by the DOS curves for the minority and majority spin levels (Figure 3) where there is no gap at the Fermi level.

Carbonylation leads to a complete quenching of the magnetic moment, rendering $[Ni_{10}Ge(CO)_{20}]^{2-}$ diamagnetic. The

(23) Rösch, N.; Sandl, P.; Görling, A.; Knappe, P. *Int. J. Quantum. Chem.* **1988**, *S22*, 275.

(24) American Institute of Physics. *Handbook*; McGraw-Hill: New York, 1963.

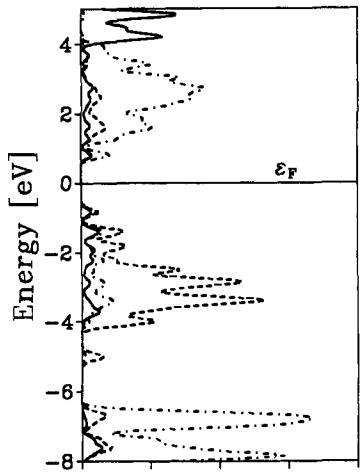

Figure 4. $[Ni_{10}Ge(CO)_{20}]^{2-}$ density of states (in arbitrary units) generated by Gaussian broadening of the one-electron energies (non-spin polarized calculation): --, Ni 3d contribution; —, Ni 4s–4p contribution, -·-, contribution of the CO orbitals. ϵ_F indicates the cluster Fermi energy (the cluster HOMO).

Table III. Average Distribution of Unpaired Electrons between Bulk and Surface Atoms in High-Nuclearity Ni Clusters

cluster	total no. of unpaired electrons	n_s[a] bulk Ni	n_s[a] surface Ni
Ni_{32}	26.44	0.74	0.86
$Ni_{32}C_6$	10.13	0.05	0.41
$[Ni_{32}C_6]^{6-}$	7.40	0.04	0.30
$Ni_{32}(CO)_{36}$	3.82	0.50	0.00
$[Ni_{32}(CO)_{36}]^{6-}$	2.50	0.36	-0.01
$Ni_{32}C_6(CO)_{36}$	0.00	0.00	0.00
$[Ni_{32}C_6(CO)_{36}]^{6-}$	0.00	0.00	0.00
Ni_{44}	32.66	0.72	0.75
$Ni_{44}(CO)_{48}$	3.37	0.56	0.00
$[Ni_{44}(CO)_{48}]^{6-}$	3.57	0.59	0.00

[a] n_s denotes the average number of unpaired electrons per atom.

HOMO–LUMO gap is about 1.5 eV (see also Figure 4). Moreover, the cluster HOMO is separated by about 1 eV from the top of the d-band, indicating a discrete structure of the one-electron energies near the Fermi level. All these data suggest that in this cluster, also, the nature of the electronic structure is entirely molecular with no trace of metallic behavior.

3.3. The Cluster $[Ni_{32}C_6(CO)_{36}]^{2-}$. This cluster is formed by a cube of eight "bulk" Ni atoms surrounded by 24 "surface" Ni atoms forming a truncated octahedron; 6 interstitial C atoms occupy the center of each Ni_8 square antiprism (Figure 1). This cluster is large enough to accommodate in the interior some Ni atoms with bulklike coordination.

A calculation on Ni_{32} in the geometry of the carbonylated form, but without any interstitial C atoms, yields a high magnetization of 26 unpaired electrons (Table III). The total DOS (Figure 5) clearly shows that the corresponding spin density is essentially localized in the 3d-band. Interestingly, a feature of dominant sp-character is found below the d-band; this has also been observed in other naked Ni clusters.[9] These occupied Ni sp-levels play an important role in determining the strength of the metal–metal bonds. But they are destabilized and shifted above the Fermi level when the CO ligands are added to the structure, due to the repulsion between the 5σ orbital of CO and the diffuse Ni 4s-derived orbitals.[25] These low-lying s-derived orbitals participate in the strong bonding of the interstitial C atoms, as can be seen from the DOS curve of the $Ni_{32}C_6$ cluster (Figure 6). However, the interstitial C atoms also induce, directly or indirectly, a substantial reorganization in the Ni 3d-level manifold with a consequent reduction of the total magnetization from 26 to 10 unpaired

(25) Bagus, P. S.; Nelin, C. J.; Bauschlicher, C. W. *Phys. Rev. B* **1983**, *28*, 5423.

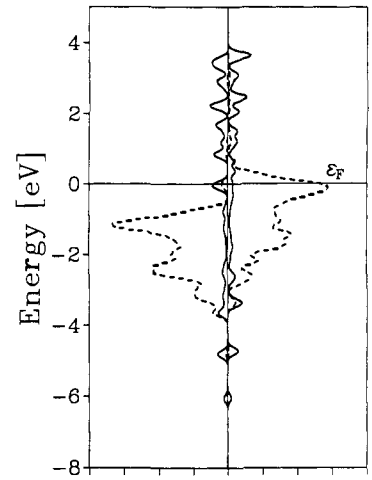

Figure 5. Ni_{32} density of states (in arbitrary units) generated by Gaussian broadening of the one-electron energies (spin polarized calculation; left side minority spin, right side majority spin): --, Ni 3d contribution; —, Ni 4s–4p contribution. ϵ_F indicates the cluster Fermi energy.

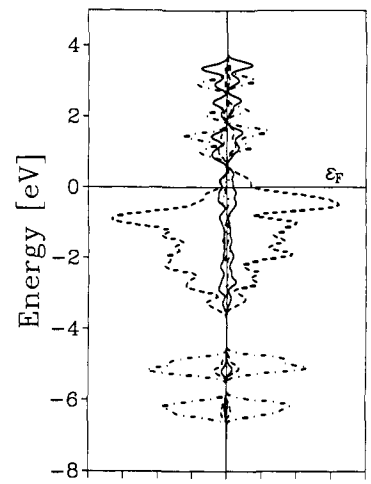

Figure 6. $Ni_{32}C$ density of states (in arbitrary units) generated by Gaussian broadening of the one-electron energies (spin polarized calculation; left side minority spin, right side majority spin): --, Ni 3d contribution; —, Ni 4s–4p contribution; -·-, contribution (×5) of the C atoms. ϵ_F indicates the cluster Fermi energy.

electrons (Table III). Quite interestingly, this decrease of the magnetic moment is not uniform and involves mainly the bulk Ni atoms, whose original magnetism is quenched almost completely, while the surface Ni atoms each still carry 0.4 unpaired electrons.

The effect of the ligand shell has been studied for both clusters, Ni_{32} and $Ni_{32}C_6$. The carbonylation of Ni_{32} results in a cluster which still has some magnetic character. About four unpaired spins are found, the corresponding spin density being entirely localized on the eight bulk Ni atoms (Table III). This result, although obtained on a structure where the removal of the interstitial C atoms leaves large empty cavities, confirms the idea that the appearance of a magnetic behavior is connected to the presence of Ni atoms not directly interacting with the CO ligands. On the other hand, when the 36 CO ligands are added to $Ni_{32}C_6$ the final cluster looses all its magnetic character. Two mechanisms contribute to the reduction of the magnetism in Ni_{32}: the interstitial C atoms quench the unpaired spin density from the internal Ni atoms and the CO ligands that of the peripheral Ni atoms.

This result is of considerable importance for the experimental study of the magnetism of giant clusters containing some hundreds of metal atoms. These neutral clusters are impossible to crystallize and are usually characterized by high-resolution transmission

Table IV. Total Number of Unpaired Electrons as a Function of the Total Charge n of the Cluster

cluster	charge $n = 0$	$n = 2$	$n = 4$	$n = 6$
$[Ni_{32}C_6]^{n-}$	10.13	8.94	8.02	7.40
$[Ni_{32}(CO)_{36}]^{n-}$	3.82	3.31	2.86	2.50
$[Ni_{32}C_6(CO)_{36}]^{n-}$	0.00	0.00	0.00	0.00
$[Ni_{44}(CO)_{48}]^{n-}$	3.37	3.42	3.49	3.57

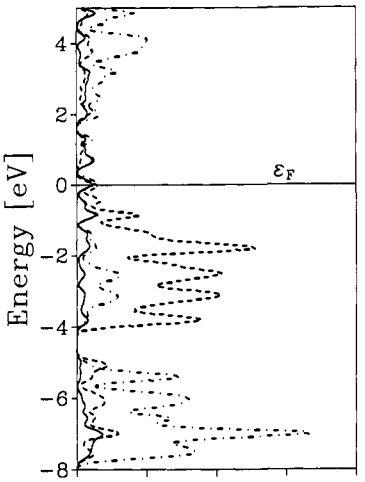

Figure 7. $[Ni_{32}C_6(CO)_{36}]^{2-}$ density of states (in arbitrary units) generated by Gaussian broadening of the one-electron energies (one-spin polarized calculation): – –, Ni 3d contribution; —, Ni 4s–4p contribution; –·–, contribution of the CO orbitals. ϵ_F indicates the cluster Fermi energy (the cluster HOMO).

electron microscopy. Therefore, it can be quite difficult to detect interstitial atoms experimentally. However, the present results show that impurity or interstitial atoms may be as efficient in quenching the magnetic moment of the metal atoms as the outer ligands.

Since the experimentally isolated Ni carbonyl clusters considered here always exist as anions,[15-18] it is important to stress that the conclusions reached so far are entirely independent of the total charge of the cluster. For values of $n = 0$, 2, 4, and 6, $[Ni_{32}(CO)_{36}]^{n-}$ and $[Ni_{32}C_6(CO)_{36}]^{n-}$ exhibit the same magnetic behavior, i.e. the one is magnetic while the other is diamagnetic (Table IV).

The DOS profile of $[Ni_{32}C_6(CO)_{36}]^{6-}$, (Figure 7) shows an increased density of levels around the Fermi level compared to the smaller clusters. Thus, although the cluster does not exhibit magnetic behavior, its electronic structure begins to resemble that of a metal, at least in some qualitative features. The cluster has no gap since three levels, t_{1u}, a_{2g}, and t_{2g}, together holding 10 electrons, are found almost degenerate near the Fermi level. However, the next level is 0.54 eV higher, indicative of the "insulating" nature of the system.

3.4. The Cluster $[Ni_{44}(CO)_{48}]^{6-}$. The cluster $[Ni_{38}Pt_6(CO)_{48}]^{6-}$ is one of the largest polynuclear complexes that has been obtained in crystalline form and characterized by X-ray diffraction.[18] The 6 Pt atoms form a regular octahedron encapsulated in a larger octahedron of 38 Ni atoms (Figure 1). The geometry of the metal core closely resembles that of an fcc (face-centered cubic) bulk metal, and the presence of metal atoms with bulk coordination makes it an ideal candidate for the study of the transition from the molecular to the metallic state. Because the Pt would have to be treated in some relativistic approximation, we have considered a model structure with a core of six Ni atoms.

The Ni–Ni distances in the real complex are scattered around the average 2.58 Å.[18] This value, which is slightly longer than in bulk Ni, was used in the calculations. This geometric factor is one reason why in Ni_{44} the average magnetization per atom, about 0.7 for bulk and surface Ni atoms (Table III), exceeds the bulk value. Upon addition of the ligands, the total number of

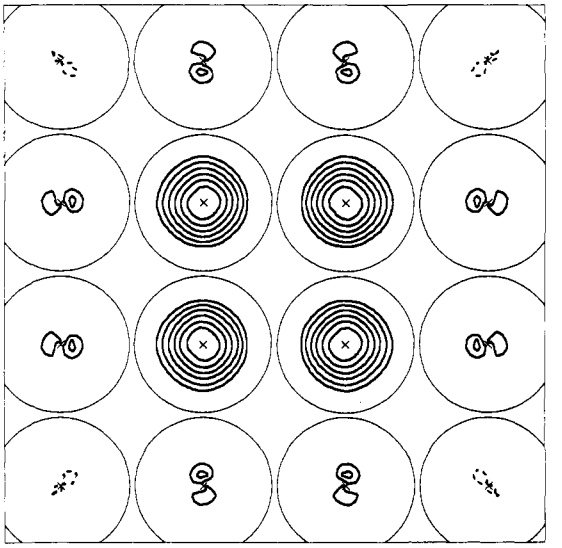

Figure 8. Electron density contour map of the difference between majority and minority spin in $[Ni_{44}(CO)_{48}]^{6-}$ computed in one of the σ_d planes of the cluster. The solid and dotted lines indicate positive and negative values, respectively. The sizes of the nickel atoms are indicated by circles tracing spheres of metallic radius.

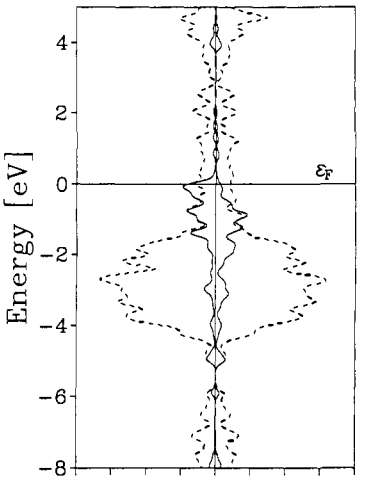

Figure 9. $[Ni_{44}(CO)_{48}]^{6-}$ density of states (in arbitrary units) generated by Gaussian broadening of the one-electron energies (spin polarized calculation; left side minority spin, right side majority spin): – –, surface Ni contribution; —, bulk Ni contribution. ϵ_F indicates the cluster Fermi energy.

unpaired spin decreases from 33 to 3. This residual magnetic moment in the carbonylated cluster contrasts with the results for the other, smaller clusters discussed so far (also including those of ref 9). Again, the size of the magnetic moment is rather independent of the charge of the cluster, it is 3.37 in neutral $Ni_{44}(CO)_{48}$ and 3.57 in $[Ni_{44}(CO)_{48})]^{6-}$ (Table IV).

This result is consistent with the experimental observation that 4.8 unpaired electrons are associated with the cluster $[Ni_{38}Pt_6(CO)_{44}]^{6-}$.[5d] In our model, we have replaced the Pt core atoms by Ni atoms, and therefore, we should not expect quantitative agreement with experimental data. But the present result provides independent complementary evidence for the fact that the presence of bulk-type metal atoms are a prerequisite for the observed magnetic behavior. In fact, the calculations show that the three unpaired electrons in the carbonylated cluster are entirely localized on the core Ni atoms and not on the surface atoms (see Table III). This may be confirmed by inspection of Figure 8, where the spin density difference (majority minus minority spin) is plotted in one of the symmetry planes of the cluster. In Figure 9, we report the DOS curves for the majority and minority spin levels of $[Ni_{44}(CO)_{48}]^{6-}$, distinguishing the contributions from bulk and surface Ni atoms. This illustrates the strong reorganization in

the electron distribution of the surface Ni atoms caused by the CO ligands. The contribution of the bulk Ni atoms closely resembles that of a bare Ni cluster, which, in turn, shows strong analogies with the bulk DOS.[26] The Fermi level cuts across the bulk Ni 3d contribution of the DOS of the cluster, a feature which is typical for metallic behavior. The major part of the surface Ni 3d DOS lies much lower in energy; the minority and majority spin components are almost exactly symmetric as a consequence of the total quenching of the magnetism on these surface atoms. The gap at the Fermi level, if any, is very small, and the one-electron spectrum nearly forms a metallic continuum around the Fermi energy. The bulk Ni atoms essentially retain their bulk configuration $3d^94s^1$ character, in contrast to the surface Ni atoms which undergo a strong rehybridization that increases their $3d^{10}$-like character.[9]

The present results show that the quenching of the Ni magnetic moment due to the CO ligands field is a relatively short-range effect and does not cancel the metallic character of bulk metal atoms. However, some reduction of the magnetization, from 0.7 to 0.6 μ_B, is found also on the six bulk Ni atoms (see Table III), indicating that some indirect quenching occurs through metal–metal interaction.

4. Conclusions

In this paper, we have presented the results of LCGTO-LDF calculations performed on high-nuclearity bare and carbonylated Ni clusters. The analysis of the results, combined with our previous study on low-nuclearity Ni clusters,[9] allows us to draw some general conclusions on the effect of the carbonylation on the properties of bare clusters, the differences between naked and carbonylated clusters, and the change of the properties as the cluster size increases.

Bare Ni_n clusters containing a few tens of atoms exhibit some of the features of the bulk metal. The average magnetization, 0.7–0.9 μ_B, is always larger than in the bulk because of the larger Ni–Ni distances and the low coordination of the Ni atoms. It is well-known[27] that the magnetic moment decreases as the average coordination of the atom increases. This is the consequence of the broadening of the bands and of the concomitant promotion of electrons from majority to minority spin bands. This effect is responsible for the 4–6% enhancement of the magnetic moment of the first layer of Ni(100) with respect to a bulk layer,[27] a feature which is reproduced in the largest Ni clusters considered here (see Table III). The average atomic configuration of the bare Ni clusters is close to $3d^94s^1$, just as in metallic Ni. The DOS profiles of Ni_{32} and Ni_{44} show two pronounced features in close analogy with the bulk DOS;[26] the appearance of a Fermi edge can also be clearly seen in the DOS curves of the largest naked clusters considered (see Figure 5 and Figure 1 in ref 28).

Low-nuclearity Ni carbonyl clusters, containing 10 metal atoms or less, can in no way be considered as "compounds containing a finite group of metal atoms which are held together entirely, mainly or at least to a significant extent by bonds between metal atoms", according to one of the original definitions of metal clusters.[29] On the contrary, there is enough evidence that the metal–metal interaction in small carbonylated Ni clusters is of a completely different nature than in the bare clusters, hence than in the metal. The main sign of this change in metal–metal interaction is the total quenching of the magnetic moment induced by the ligands.

The detailed mechanism of the interaction of CO with a transition metal atom, which is the origin of the large electronic rearrangement within the metal cluster, has been analyzed in detail in several investigations and is now commonly accepted.[25,30] The interaction between the diffuse 5σ lone pair of CO and the outer sp orbitals of the metal is purely repulsive.[25] In order to reduce this repulsion the metal atom rehybridizes, increasing its d-character. In Ni this corresponds to a change in the configuration from $3d^94s^1$ to formally $3d^{10}$ with complete quenching of the 3d spin density. This is not too surprising if one considers that, even though in the free Ni atom the $^1S(3d^{10})$ state is almost 5 eV above the $^3D(3d^94s^1)$ state, $Ni(CO)_4$ is a diamagnetic molecule where Ni has a $3d^{10}$-like configuration.[31]

As the size of the cluster grows, metal atoms with typical bulk coordination can be accommodated in the structure. These internal Ni atoms are only slightly perturbed by their interaction with the matrix of the ligands. Therefore, they retain part of their original magnetic character. They are responsible for the weak metallic magnetic behavior observed both theoretically and experimentally[5] on high-nuclearity Ni clusters. According to this picture, high-nuclearity cluster compounds can be viewed as systems containing a core of metal atoms (perhaps small), held together mainly by metal–metal bonds surrounded by a "shell" of weakly interacting metal atoms whose structure is deeply modified by the interaction with the ligand environment. The ratio between the number of bulk atoms and the surface atoms in the cluster core will determine whether the behavior of the material is to be viewed as more molecular or more metallic.

Acknowledgment. We thank P. S. Bagus, IBM Almaden Research Center, for critically reading this manuscript. This work has been supported by the Deutsche Forschungsgemeinschaft through Grant SFB 338 and by the Fonds der Chemischen Industrie.

(26) Moruzzi, V. L.; Janak, J. F.; Williams, A. R. *Calculated Electronic Properties of Metals*; Pergamon Press: New York, 1978.

(27) (a) Jepsen, O.; Madsen, J.; Andersen, O. K. *Phys. Rev. B* **1982**, *26*, 2790. (b) Krakauser, H.; Freeman, A. J.; Wimmer, E. *Phys. Rev. B* **1983**, *28*, 610. (c) Liu, F.; Press, M. R.; Khanna, S. N.; Jena, P. *Phys. Rev. B* **1988**, *38*, 5760.

(28) Rösch, N.; Ackermann, L.; Pacchioni, G.; Dunlap, B. I. To be published.

(29) Cotton, F. A. Q. *Rev. Chem. Soc.* **1966**, 416.

(30) (a) Walch, S. P.; Goddard, W. A. *J. Am. Chem. Soc.* **1976**, *98*, 7908. (b) Rives, A. B.; Fenske, R. F. *J. Chem. Phys.* **1981**, *75*, 1293. (c) Basch, H.; Cohen, D. *J. Am. Chem. Soc.* **1983**, *105*, 3856. (d) Koutecky, J.; Pacchioni, G.; Fantucci, P. *Chem. Phys.* **1985**, *99*, 87. (e) Ha, T. K.; Nguyen, M. T. *J. Mol. Struct. (THEOCHEM)* **1984**, *109*, 331. (f) Jeung, G. H.; Koutecky, J. *Chem. Phys. Lett.* **1986**, *129*, 569.

(31) (a) Bauschlicher, C. W.; Bagus, P. S. *J. Chem. Phys.* **1984**, *81*, 5889. (b) Jörg, H.; Rösch, N. *Chem. Phys. Lett.* **1985**, *120*, 359.